Forces in a Moving Bed of Particulate Solids with Interstitial Fluid Flow

HERMAN L. BRANDT and BENJAMIN M. JOHNSON

Hanford Atomic Products Operation, General Electric Company, Richland, Washington

The use of granular solids flowing as a consolidated or dense phase has had wide application in processes utilizing the moving bed principle, such as the Houdryflow and T.C.C. catalytic cracking units. More recently there has been considerable effort to design continuous countercurrent solid-liquid contactors for applications such as ion exchange. One scheme (2) involves the movement of a consolidated bed of resin countercurrent to fluid flowing through a portion of the bed. The bed is moved by force transmitted through the particles. The origin of the force may be either a fluid flowing concurrently through another portion of the bed or a piston (bellows) arrangement acting directly on the solids.

The work reported here is an outgrowth of efforts to develop a continuous, dense bed, countercurrent resin contactor. Difficulty in achieving a stable condition for countercurrent flow of resin and fluid prompted a study of the solid stresses that develop during both concurrent and countercurrent flow to determine the utility of an analysis by Jury (2) of the forces required for resin movement. His work is the only investigation of solid stresses in consolidated, particulate beds through which a fluid is flowing. Delaplaine (1) made a comprehensive study of forces acting in granular solids flowing downward under the influence of gravity. His work considered neither the movement of solids under the influence of fluid flow nor the movement of solids counter to gravity or other body forces.

STRESS THEORY

The force distribution in flowing bulk solids is very difficult to analyze rigorously and is not directly comparable to a fluid system. The resistance to flow of one particle past another or past the stationary wall of the container does not follow the laws of fluid motion but is governed by the behavior of solid friction. The presence of a fluid flowing through the solid does not change the intrinsic properties of the system if the particles remain in contact with one another and are not fluidized. The pressure drop of the fluid can be incorporated in the analysis of forces as an additional body force similar to that of gravity. Figure 1 shows the stresses (in cylindrical coordinates) acting on a differential volume of a bed of solids. There are three normal compressive stresses, σ_z, σ_θ, σ_r, acting perpendicular to the planes and six shear stresses, τ_{rz}, $\tau_{r\theta}$, etc., acting parallel to the plane of the stress in the direction of the second subscript. Stress is distributed by particle-to-particle friction. No equilibrium shear stress can exist in excess of that determined by the internal bed friction. Thus for example if the ratio τ_{zr}/σ_z becomes equal to or greater than the coefficient of internal friction μ, slipping will occur along the z plane and the stress pattern will be altered throughout the system.

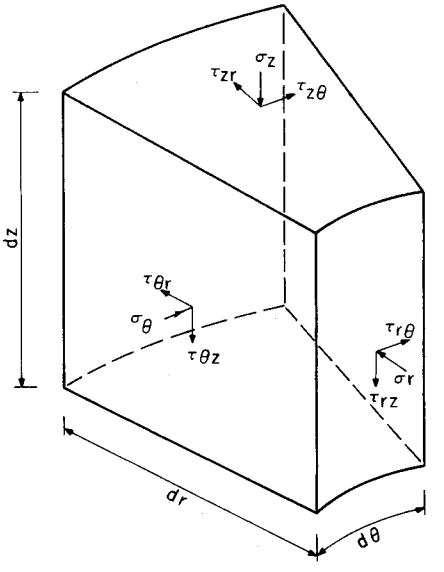

Fig. 1. Forces acting on a differential volume in cylindrical coordinates.

Jenike (4) presented a mathematical development of the conditions of flow of bulk solids from vertical and converging channels for the case of no interstitial fluid flow and essentially zero velocity. His results predict the onset of solids flow but do not indicate the force distribution during flow.

The forces acting at the boundaries of a bed are of particular interest. These boundary forces are the radial and shear stress at the wall and the average vertical stress over the cross section of the containing vessel (Figure 2). Delaplaine (1) measured the stresses acting both at the boundaries and within downward flowing beds of sand, glass beads, and bead catalysts. His results for flowing beds are similar to those for static beds (5, 6, 7) in that the stresses are not proportional to bed depth but increase asymptotically to constant values at bed depths greater than roughly four to six tube diameters.

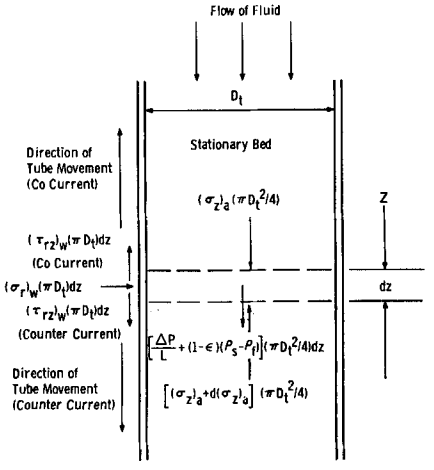

Fig. 2. Force balance of boundary and average stresses.

This behavior for the radial stress at the wall and the average vertical stress is to be expected from consideration of a force balance of the average stresses on a differential section across the tube as shown in Figure 2. A vertical force balance on this horizontal slab gives

$$\frac{d(\sigma_z)_a}{dz} = \rho_b - \frac{4(\tau_{rz})_w}{D_t} \tag{1}$$

Substitution of the stress ratios $\mu' = (\tau_{rz})_w/(\sigma_r)_w$ and $k_a = (\sigma_r)_w/(\sigma_z)_a$ yields

$$\frac{d(\sigma_z)_a}{dz} = \rho_b - \frac{4k_a\mu'(\sigma_z)_a}{D_t} \tag{2}$$

If k_a and μ' are assumed constant, the solution to this equation, as developed by Janssen (3), is

$$(\sigma_z)_a = \frac{\rho_b D_t}{4k_a\mu'}\left(1 - e^{-4k_a\mu' z/D_t}\right) \tag{3}$$

Thus the average vertical stress $(\sigma_z)_a$ should approach an asymptotic value of $(\rho_b D_t/4k_a\mu')$ in deep beds. Most investigations of solid stresses, which have been limited to boundary measurements in static systems (5, 6, 7), have correlated the results by the Janssen equation with a constant value k_a and μ' assumed. Delaplaine's results indicate that for a shallow bed, that is the region in which $(\sigma_z)_a$ and $(\tau_{rz})_w$ are rapidly varying with bed depths, these stress ratios are not constant. Generally k_a increased from a value of about 1.0 at the top of the bed to about 1.8 in deep beds, while μ' decreased by about 15 to 45% over the same span.

In an unconfined bed the ratio of horizontal-to-vertical stress is given by

$$\frac{\sigma_r}{\sigma_z} = k = \frac{1 - \sin\phi}{1 + \sin\phi}$$

where ϕ is the angle of internal friction, that is $\phi = \tan^{-1}\mu$. The internal friction coefficient μ is the dynamic frictional resistance of the particles within the granular bed to flow past one another. Consequently the angle of internal friction ϕ is for example the angle with the horizontal assumed by the moving core of solids in a vessel provided with a central opening in the bottom. The above equation indicates that the ratio of radial to vertical stress k is never greater than unity. However, k_a can be greater than 1 because shearing occurs in the outer region of the bed because the velocity of the particles at the walls is slightly lower than that in the center of the bed, which moves as a rodlike core. The shearing causes a rapid increase in radial stress in the region between the core, where σ_r is independent of radial position, and the wall.

Fluid flow through a moving bed of particulate solids does not change the basic behavior of the system. It does however alter some of its flow properties. The fluid exerts a drag on the solids which can be treated as a body force on the bed as a continuum. This force can be included with terms involving the bulk density of the solids if the bed is moving in a vertical direction. The flowing fluid alters the internal friction of the particles and consequently affects the maximum shear stress that can exist. The angle of repose of the particles and coefficient of friction between the bed and the restraining surfaces are also affected.

Jury (2) analyzed the transmittal of force by resin solids through which fluid was flowing and developed equations for cocurrent and countercurrent flow. The equation for cocurrent flow may be rearranged to be essentially the same as the Janssen equation. Thus for cocurrent movement

$$(\sigma_z)_a = \frac{AD_t}{4k_a\mu'}\left(1 - e^{-4k_a\mu' z/D_t}\right) \tag{4}$$

and for countercurrent movement

$$(\sigma_z)_a = \frac{AD_t}{4k_a\mu'}\left(e^{4k_a\mu' z/D_t} - 1\right) \tag{5}$$

where

$$A = \frac{\Delta P}{L} + (1 - \epsilon)(\rho_r - \rho_l)$$

In his analysis Jury assumed the value of k_a was 1 and μ' was constant.

Equation (4) applies if the net body force, indicated by the term A, acts in the same direction as the movement of the bed relative to the tube, while Equation (5) applies if the force A acts in the opposite direction as the movement of the bed. These equations apply only to packed beds, that is a contiguous bed of solids. For concurrent flow upward and countercurrent flow downward one must consider the possibility of fluidizing the bed. Under these conditions the resin stress is zero at every point. If the particles are constrained as a packed bed, the situation is equivalent to that investigated in this paper.

In the work reported here point values for the particle-to-wall friction coefficient μ' and the ratio of the radial-to-vertical boundary stresses $(\sigma_r)_w/(\sigma_z)_a = k_a$ were determined through use of the appropriate differential force balance comparable to Equation (2). Thus for cocurrent movement

$$\frac{d(\sigma_z)_a}{dz} = A - \frac{4k_a\mu'(\sigma_z)_a}{D_t} \quad (6)$$

and for countercurrent movement

$$\frac{d(\sigma_z)_a}{dz} = A + \frac{4k_a\mu'(\sigma_z)_a}{D_t} \quad (7)$$

One can see from the term A in these equations the manner in which the pressure drop of the fluid flowing through the solids is incorporated with the body force exerted in the bed owing to gravity.

EXPERIMENTAL METHODS

Apparatus

The equipment provided a means of measuring the average vertical stress $(\sigma_z)_a$ and the radial stress $(\sigma_r)_w$ at the wall of the tube containing a bed of particulate solids during movement of the bed cocurrent and countercurrent to the direction of liquid flow. Water was pumped down through the bed by a positive displacement rotary pump, and the pressure drop was recorded by an aneroid manometer recorder. The two directions of movement were simulated by driving the 4-in. diameter, 4-ft. high Lucite tube, which was bolted to a rack mounted on

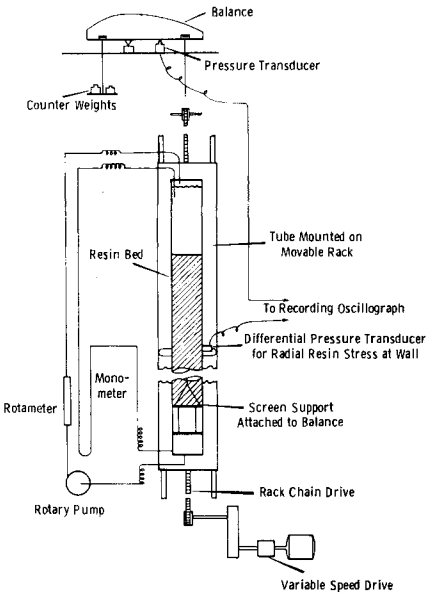

Fig. 3. Schematic diagram of equipment.

tracks, either up or down at a constant, preselected velocity by a chain and sprocket arrangement as shown in Figure 3.

The bed was supported by a 20 × 150 mesh Dutch Twill stainless steel screen which was fixed to a ring or piston of Teflon ⅜ in. high and 3-15/16 in. I. D. The piston in turn was bolted to a stainless steel spacer with lips for stability. A spring-loaded Teflon piston ring prevented solid particles from falling below the piston.

The average vertical stress in the bed was obtained by measuring the force exerted on the retaining screen. The screen was attached to a specially fabricated balance which had a capacity of more than 50 Kg. and a sensitivity of less than 1 g. Except for the bearing parts, it is made of aluminum. The base of the balance accommodated a load cell for transmitting the variations in force within the bed that were expected from the stick-slip movement between the solid particles and the tube wall. The supporting piston was attached to one side of the balance, and a pan was attached to the other side for holding counterweights.

Since the screen constrains the bed, it distorts the radial stress near the screen to an extent depending on the internal friction of the bed. If the bed has significant internal friction, a correction must be applied to obtain the true average vertical stress. The correction was negligible for most of the runs made. This situation was an inherent limitation in this method which could have been avoided if only cocurrent flow were of interest, by using the methods of Delaplaine (*1*), but appeared to be a convenient way to investigate stresses in countercurrent flow.

Radial stress in the resin at the tube wall was measured with a Statham differential pressure transducer. Its 1/4-in. diaphragm was mounted flush in the tube wall. The water pressure on the diaphragm was counterbalanced by pressure from a screened tap opposite the transducer. Since the rear face of this instrument could not tolerate water, air was entrapped in the horizontal tube between it and the tap.

The pressure transducers at the balance and in the tube wall were connected to a recording oscillograph. The galvanometer-light beam combination of the oscillograph was not limited by inertial effects, an important consideration in studying the sticking and slipping of the solids. The oscillograph also had the ability to record simultaneously signals from both pressure-measuring devices.

Procedure

Scope of Measurements. The radial stress at the wall of the tube and the average vertical stress across the cross section of the tube were measured for three sizes of ion-exchange resin beads and one size of glass beads moving cocurrently and countercurrently to the flow of water through the bed. Permutit SK resin nitrate form in the size ranges of 10 to 20 mesh and 20 to 40 mesh, Dowex 50 nitrate form in the 50 to 100 mesh size, and glass beads in the 20 to 50 mesh size were studied. Fluid flow sufficient to give a pressure drop up to 1.1 lb./sq. in./ft. of resin bed were used. The velocity of the moving bed of solids was varied from 1 to 30 cm./min.

Only one tube diameter was used, which seemed justified in this limited study. The results of Delaplaine indicated that if the ratio of tube-to-particle diameter is greater than 50, the tube diameter has no effect on the coefficient of friction or the stress ratio k_a.

No runs were made with the resin out of water since the characteristics of the beads change when dry.

A run consisted of measuring the vertical stress for a particular bed height and the variation in radial stress over the entire bed. The resin was treated with nitric acid and rinsed with distilled water; only distilled water was used during stress measurements. The particles were initially fluidized to remove any fines that had been formed and allowed to settle. They were then packed by pumping water at high velocity through the bed. At the start the tube was positioned so that the bed was 3 to 5 cm. above or below the radial stress transducer to permit adjustment of water flow and to allow the bed to attain steady state before measurements were taken. To obtain the total vertical force on the bed sufficient counterweight was placed onto the left-hand balance pan to keep the recorder trace of the load cell within the required limits. The average force from this trace was added to the counterweight. The sum was then divided by the area of the bed cross section to give the average vertical stress $(\sigma_z)_a$. The radial stress at the wall $(\sigma_r)_w$ was taken directly from the trace.

A small tube from the water tap shown in Figure 3 permitted measuring the pressure drop with bed height as the tap moved with respect to the bed. Thus, when compressibility of resin or accumulation of fines near the screen was suspected, the linearity of pressure drop could be checked.

CONCURRENT MOVEMENT

Measured values of the radial stress at the wall $(\sigma_r)_w$ and the average vertical stress $(\sigma_z)_a$ were used to evaluate the ratio of these two stresses designated as k_a and the wall friction coefficient μ'. During the early phases of the work these were obtained by measuring the slope of the curve of $(\sigma_z)_a$ vs. bed height z curve from which $k_a\mu'$ could be calculated, from Equation (6), while the stress ratio k_a was determined from the point values of $(\sigma_r)_w$ and $(\sigma_z)_a$. However observation of the trend in k_a in go-

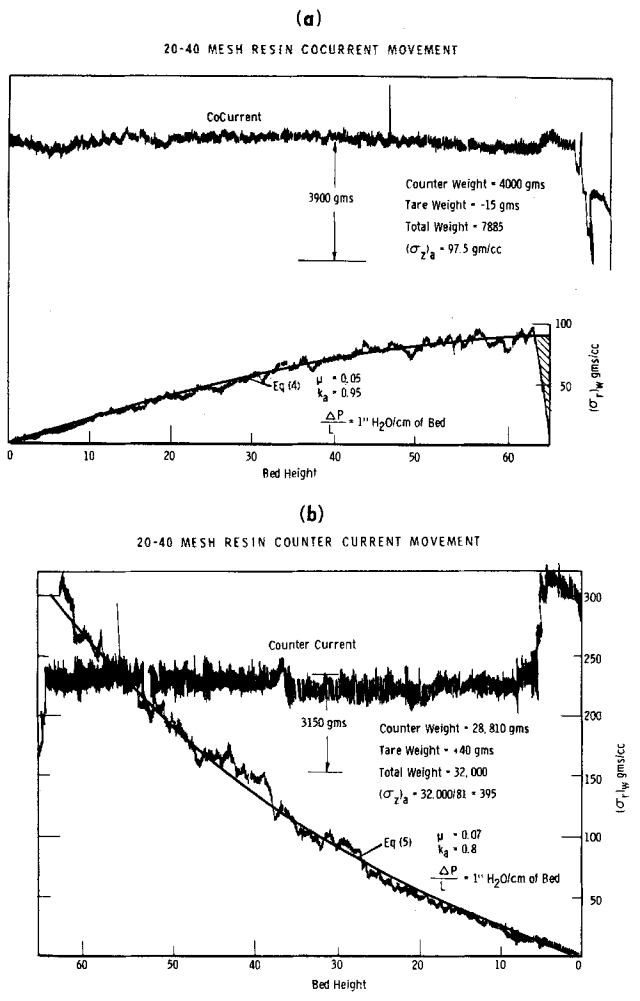

Fig. 4. Typical plot of radial and vertical stresses.

ing from shallow to deep beds indicated μ' and k_a could be determined from the asymptotic value of the average vertical stress, $(\sigma_z)_{a,d}$ (that is in a deep bed) and a complete curve of $(\sigma_r)_w$ vs. bed depth z. It was noted that k_a varied nearly linearly with the ratio $(\sigma_r)_w/(\sigma_r)_{w,d}$, that is the ratio of the point value of the radial stress at the wall to the asymptotic (deep bed) value of this stress. Thus since the value of k_a at zero bed depth ($k_{a,0}$) was known from the initial slope of the $(\sigma_r)_w$ vs. z curve, and $k_{a,d}$ was equal to $(\sigma_r)_{w,d}/(\sigma_z)_{a,d}$, a satisfactory approximation of k_a over the range of bed depths could be calculated without the necessity of making several runs to determine $(\sigma_z)_a$ vs. z. This trend in k_a is similar to that noted by Delaplaine (*1*).

The variation in radial and vertical stress with bed height was somewhat different for the four classes of solids studied. Figure 4*a* is an actual trace of the strain gauge output made on the recording oscillograph measuring $(\sigma_r)_w$ for 20 to 40 mesh resin. It shows variation in radial stress at the wall as the depth of bed increased. Also recorded is the output of the pressure transducer activated by the balance to which the supporting screen was attached. This measured the total vertical force exerted by the bed from which $(\sigma_z)_a$ at the total depth of the bed was calculated. Figure 4*b* is a similar trace during countercurrent movement and is discussed below. The behavior of the 20 to 40 mesh resin was closely predicted by the solution of the differential force balance, Equation (4), with constant values assumed for μ' and k_a. The solid line in Figure 4*a* is the plot of Equation (4) with $\mu' = 0.05$ and $k_a = 0.95$. This value for μ' compares closely with an approximate value of 0.06 measured by Hancher and Jury (*2*) between Dowex 50 resin and a cadmium plated surface. However they subsequently estimated from flow data that the value of μ between resin and glass was more nearly 0.009.

The behavior of 50 to 100 and 10 to 20 mesh resin was not so well ordered. Figure 5 is a plot showing the variation of $(\sigma_r)_w$ and $(\sigma_z)_a$ for these two sizes of resin moving concurrent to water flowing at a pressure drop of 2.54 (g./sq.cm.)/cm. of bed. For the 50 to 100 mesh resin the stress ratio k_a was not constant but increased from 1 for very shallow beds to about 1.3 in beds deeper than about three tube diameters. In this respect it differed from the other two resin sizes for which k_a values were less than 1 or very nearly equal to 1. An increase in k_a as bed depth increased was also noted with the glass beads. This confirms the results of Delaplaine in moving beds of dry solids (*1*). Another difference in the data for 50 to 100 mesh resin was the inconsistent behavior of the radial stress $(\sigma_r)_w$ in shallow beds. Generally the variation with bed depth indicated μ'_0 (wall friction at zero bed depth) to be about 30% greater than the asymptotic value μ'_d (deep beds); some runs however indicated μ'_0 to be about 40% less than μ'_d. This wide variation in μ'_0 may have been the result of differences in the initial packing within the bed. The variation in k_a with bed height was consistent in all runs as was the value of μ'_d.

For the 10 to 20 mesh resin, μ'_d varied significantly with the length of time since the resin had been in contact with nitric acid. Nitrated resin which had been less than 3 hr. in distilled water had essentially the same flow properties as the 20 to 40 mesh resin. Resin in contact with water longer than a week exhibited a reproducible value of μ'_d more than four times as great as that of the 20 to 40 mesh resin. The value of k_a for new 10 to 20 mesh resin was almost independent of bed depth, while k_a for old resin decreased from 1.0 at zero bed depth to 0.7 in deep beds.

The 20 to 50 mesh glass beads were studied to tie in this work with that of Delaplaine on downward flowing

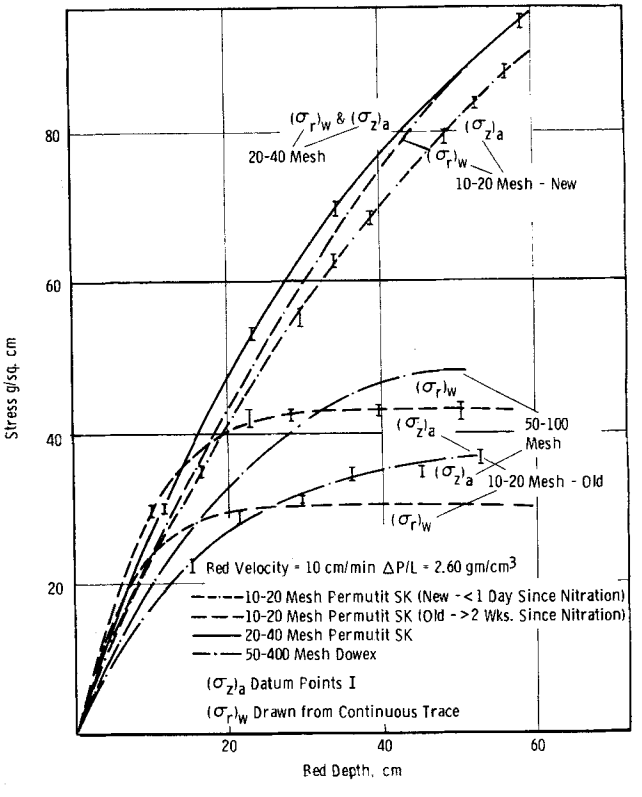

Fig. 5. Effect of bed depth on vertical and radial stress.

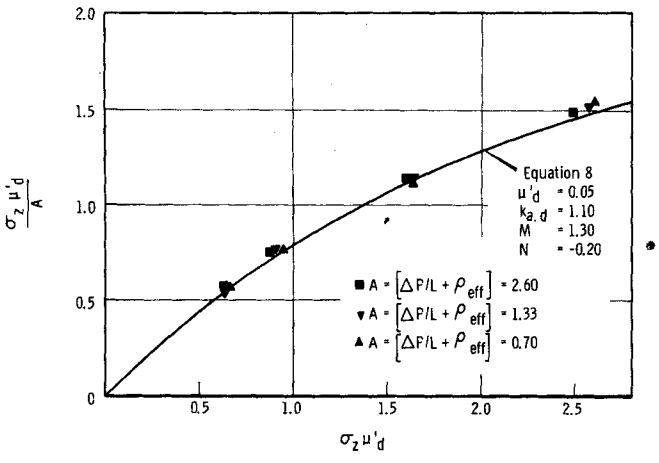

Fig. 6. Comparison of Equation (8) with data for 10 to 20 mesh resin.

beds of dry solids (*1*). The value of μ'_d between glass beads in water and the Lucite tube was 0.22. Delaplaine calculated a value of 0.17 between dry beads and a steel tube. In the present system $k_{a,d}$ was 1.5 compared with 2.0 in the dry system. This decrease in k_a indicates that the flow of fluids through the bed reduces the lateral force in the region of pronounced shearing. Possibly the fluid drag increases the ease with which particles can move to fill local voids that continually form in the region of shearing as the bed moves. Greater voids would indicate that greater lateral thrust is required to force individual beads past one another. Qualitatively it was noted that the tendency for the top of the bed to become dished because of a lower velocity at the walls was less marked for solids with low values of k_a. In all cases the level of solids at the periphery was never greater than about 5 mm. after several feet of travel. This is in contrast to Delaplaine's observation that the top of the bed had to be continually leveled during the runs with dry solids.

Initially runs were made at various values of $\Delta P/L$, the pressure drop per unit length of bed. This pressure drop was indicative of the fluid velocity relative to the bed; that is it was exclusive of the hydrostatic head. At the low fluid velocities involved the fluid shear stress at the tube wall was negligible. Data on the average vertical stress $(\sigma_z)_a$ obtained at various bed depths and pressure drops were used as follows to demonstrate that μ' and k_a were essentially independent of $\Delta P/L$. As mentioned previously, k_a varied nearly linearly with the ratio $(\sigma_r)_w/(\sigma_r)_{w,d}$. Within the limit of experimental precision $k_a\mu'$ could be similarly expressed as a linear function of $(\sigma_r)_w/(\sigma_r)_{w,d}$ or $(\sigma_z)_a/(\sigma_z)_{a,d}$, as for example

$$k_a\mu' = \left[M + N \frac{(\sigma_z)_a}{(\sigma_z)_{a,d}} \right] \mu'_d$$

If this expression is substituted into Equation (6), the integrated result is

$$(\sigma_z)_a = \frac{pq}{p - qe^{-rz}} (1 - e^{-rz}) \qquad (8)$$

where

$$p = \frac{AD}{\mu'_d} \left[\frac{-1}{8N(M+N)} \right] [M + \sqrt{M^2 + 4N(M+N)}]$$

$$q = \frac{AD_t}{\mu'_d} \left[\frac{-1}{8N(M+N)} \right] [M - \sqrt{M^2 + 4N(M+N)}]$$

$$r = \frac{4\mu'_d}{D_t} \sqrt{M^2 + 4N(M+N)}$$

Thus a plot of $\frac{(\sigma_z)_a \mu'_d}{A}$ vs. $\mu'_d z$ should result in a single line for a particular resin if μ' and k_a were independent of A. Figure 6 is such a plot for recently nitrated 10 to 20 mesh resin. The solid curve is Equation (8) with the particular values of N, M, μ'_d, and $k_{a,d}$ indicated.

The coefficient of friction was not independent of resin velocity as might be suspected. This coefficient increased about 25% for the 20 to 40 mesh resin as its velocity increased from zero to 30 cm./min. as shown in Figure 7. However μ'_d was essentially independent of the fluid pressure drop through the bed and hence also independent of the relative fluid-to-resin velocity. A possible explanation for these observations is that since the Reynolds number was relatively low for all of the runs $\left(\text{less than } N_{Re} = \frac{D_P G_o}{\mu} \frac{1}{1-\epsilon} = 7\right)$, the width of the laminar region next to the wall was probably sufficiently thick that a particle moving at the wall would be moving through a fluid at very low velocity. Increasing the resin velocity above the local fluid velocity would therefore increase the drag for these peripheral particles.

COUNTERCURRENT MOVEMENT

Measurement of both $(\sigma_r)_w$ and $(\sigma_z)_a$ for the resin moving countercurrent to the flow of fluid indicated that μ', the coefficient of friction, and k_a, the ratio of $(\sigma_r)_w/(\sigma_z)_a$, were constant in both shallow and deep beds. Consequently the stress variation is well represented by Equation (5), and the data were treated by rearranging Equation (5) into the form

$$\ln \left[1 + \frac{(\sigma_r)_w}{A} \left(\frac{4\mu'}{D_t} \right) \right] = \left(\frac{4\mu'}{D_t} \right) k_a z$$

The term in brackets was plotted vs. z on semilogarithmic paper for various assumed values of μ' until a straight line through the origin was obtained, Figure 8. The slope

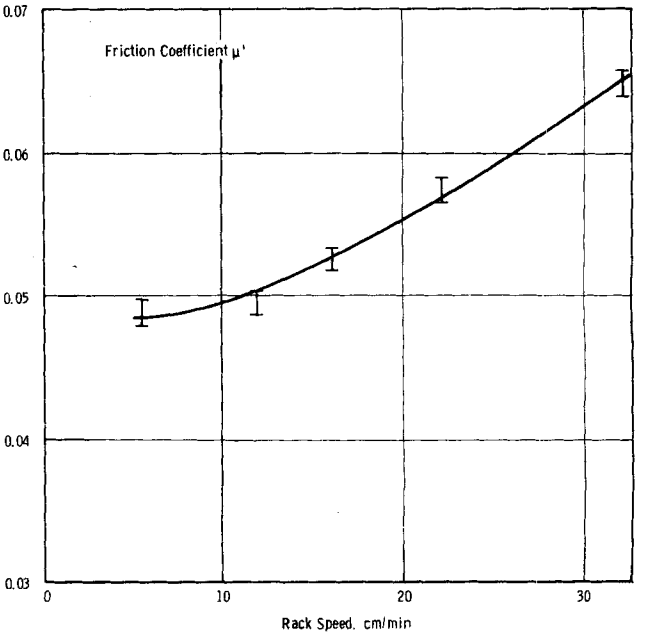

Fig. 7. Effect of resin velocity on friction coefficient concurrent movement of 20 to 40 mesh resin.

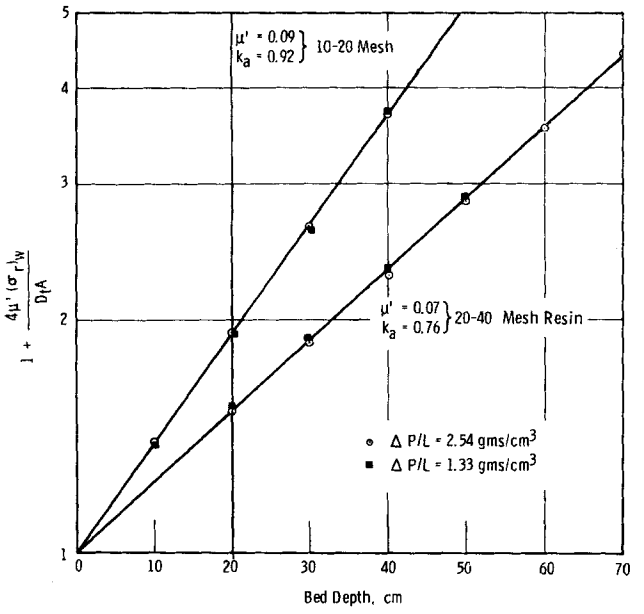

Fig. 8. Comparison of Equation (5) with experimental data.

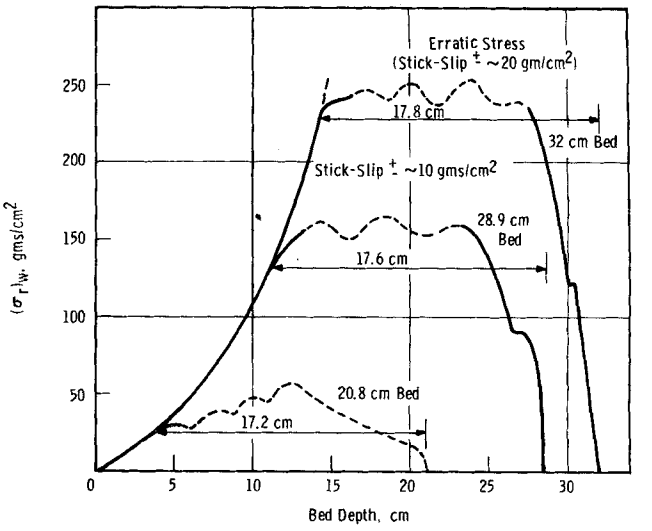

Fig. 9. Radial stress variation of 20 to 50 mesh beads showing effect of internal friction.

was then $k_a\left(\frac{4\mu'}{D_t}\right)$ from which k_a could be evaluated.

Figure 4*b* is an actual trace of the strain gauge output made on the recording oscillograph measuring $(\sigma_r)_w$ for 20 to 40 mesh resin moving countercurrent to the fluid flow. The output of the pressure transducers indicating the force on the supporting screen is also recorded on the trace shown in Figure 4*b*. The solid line is Equation (5) with $\mu' = 0.07$ and $k_a = 0.8$.

For all three sizes of resin k_a and μ' were relatively consistent for all runs at the values shown in Table 1. As in the case of cocurrent resin and fluid flow the values of these parameters were independent of the pressure drop through the bed. This is shown in Figure 8 by the fact that data points calculated from traces of $(\sigma_r)_w$ made at two different values of $\Delta P/L$ essentially coincide. This data also demonstrate that μ' (and also k_a) is independent of $(\sigma_r)_w$ despite the very high stress that can be developed during countercurrent movement which might tend to flatten the beads against the tube wall. However k_a is smaller than, and μ' is larger than, the corresponding cocurrent values. Presumably this is because of the difference in the velocity gradient of the fluid at wall in the two cases. The gradient was much steeper with cocurrent movement since tube and fluid were moving in opposite directions. Thus the tendency for a particle to roll along the wall would be greater. This would result in lower sliding drag but a greater transmission of force in the radial direction because of the greater shearing between two layers of particles. The existence of lower k_a and higher μ' in countercurrent than in cocurrent movement was noted in all three resin size classes as is indicated in Table 1.

EFFECTS OF INTERNAL FRICTION

The runs with glass beads point up the effect of internal friction on the stress pattern within the bed. The variation in $(\sigma_r)_w$ with bed depth is consistent with Equation (5) for that portion of the bed greater than approximately 17 cm. from the support screen. At this point a discontinuity in the stress pattern occurs as shown in Figure 9, and $(\sigma_r)_w$ is very nearly constant for the rest of the bed except in the immediate vicinity of the screen.

This stress pattern is the general one for granular materials, and the length-to-diameter ratio of 1.7 at the discontinuity is essentially equal to the tangent of the angle of internal friction. The region of discontinuity was not noted in the case of the resin beads as these materials exhibited almost no internal friction in flowing water. Zenz (8) indicated that the angle of internal friction could be determined from the length-to-diameter ratio of the longest bed of the granular material that could be pushed up through a tube. For materials with a low coefficient of friction with the tube wall this method would

TABLE 1. SUMMARY OF RESULTS

Concurrent movement @ 10 cm./min.

Bed material	10 to 20 mesh resin				20 to 40 mesh resin	50 to 100 mesh resin	20 to 50 mesh glass beads
Age since nitration	<3 hr.	~24 hr.	3 to 5 days	>2 wk.			
μ'_d	0.050	0.083	0.12	0.20	0.050	0.13	0.22
μ'_o	0.065	0.10	0.07	0.18	0.050	0.17	0.23
$k_{a,d}$	1.10	1.06	0.93	0.70	1.00	1.3	1.4
Countercurrent movement @ 10 cm./min.							
μ'_d		0.10	0.14		0.070	0.14	0.24
$k_{a,d}$		0.88	0.70		0.76	1.1	1.5

not be applicable since the required force for pushing would build up exponentially but at a slow rate.

In cocurrent flow the discontinuity in radial stress 17 cm. from the screen was also noted. This cohesive property of the solids results in erroneous values for $(\sigma_z)_a$ because the restraining influence of the screen distorts the radial stress pattern. In the case of cocurrent flow $(\sigma_z)_{a,\text{ measured}}$ is too high since less of the weight is supported by the column walls. The reverse is true for countercurrent flow. Measured values are corrected as follows for cocurrent movement:

$$(\sigma_z)_{a,\text{ measured}} - (\sigma_z)_{a,\text{ actual}} = \frac{2\mu'}{R}\int_o^{L'} [(\sigma_r)_{w^*} - (\sigma_r)_{w,\text{ measured}}]\, dl$$

An example of the extent of this correction can be seen as the cross-hatched areas under the stress curve in Figure 4*a*.

Anomalous behavior in the vicinity of the retaining screen was exhibited by the 50 to 100 mesh resin, and to a slight extent by the 20 to 50 and 10 to 20 mesh resins. Radial stress increased very markedly about 3 cm. above the screen in countercurrent movement with 50 to 100 mesh resin. This may have been the result of a dead-water region near the outer edge of the screen where it was attached to the piston.

The results of this study tend to confirm the correctness of Jury's analysis of resin stress. One may therefore be led to conclude, as did Jury, that countercurrent movement of resin can be accomplished by particle to particle transmission of force. Nonetheless a realization of such movement in practice is difficult, if not infeasible. The disrupting of the stress pattern due to the withdrawal of the liquid stream dissipates to a large extent the resin stress developed by concurrent flow which was counted on to force the resin countercurrent to the flow of a process stream.

SUMMARY

Boundary stresses in moving beds of solids through which a fluid is flowing have been measured. In countercurrent flow the coefficient of friction and the stress ratio were essentially independent of bed depth, and consequently the variation of radial stress at the wall and the average vertical stress were closely represented by the integrated equation of the force balance on a cross section of the bed, Equation (5). In cocurrent flow the stress variation of only the 20 to 40 mesh resin could be represented by the integrated force balance equation, Equation (4). With the other two sizes of resin the coefficient of friction μ' and the stress ratio k_a change as the bed depth increased but reached asymptotic values in deep beds.

The coefficient of friction appears to be a function of particle size, although differences in composition of the Permutit and Dowex resins may be the primary variable. The coefficient of friction μ' of the nitrated 10 to 20 mesh resin varied widely with time in distilled water. For recently nitrated 10 to 20 mesh resin, μ' was essentially equal to that for 20 to 40 mesh resin, for old 10 to 20 mesh resin μ' was about four times as great. The smaller resins exhibited no variation in friction characteristics with age since nitration.

The coefficient of friction was dependent on solid velocity; μ' increased about 25% as the bed velocity was increased from zero to 30 cm./min. However μ' was independent of the fluid velocity through the bed.

The force exerted on the bed by the flowing fluid can be treated as an additional body force and incorporated in with terms involving the bulk density of the bed. However one is generally not correct in assuming that μ' and k_a are independent of bed depth or that k_a is equal to unity.

The flowing fluid does reduce the radial-to-vertical stress ratio as the result of cutting down the resistance to shearing between particles within the bed.

The resin bed had essentially no internal friction. However the bed of glass beads had considerable internal friction which greatly affected the stress pattern in the vicinity of the supporting screen.

NOTATION

A = $\frac{\Delta P}{L} + (1-\epsilon)(\rho_r - \rho_l)$

D_P = particle diameter

D_t = tube diameter

G_o = superficial mass velocity

k = ratio of radial stress to vertical stress σ_r/σ_z

k_a = ratio of radial stress at the wall to average vertical stress = $(\sigma_r)_w/(\sigma_z)_a$

L = length of bed

L' = length of bed over which deviation from the usual radial stress pattern occurred due to internal friction with the bed.

$\frac{\Delta P}{L}$ = pressure drop per unit length of bed

r = radial distance

z = vertical distance or bed depth

Greek Letters

ϵ = void fraction

θ = angular coordinate

μ = stress ratio τ_{rz}/σ_r = coefficient of internal friction if shearing occurs perpendicular to r

μ = fluid viscosity when used in conjunction with the Reynolds number

μ' = coefficient of friction of solids on the container wall

ρ_b = bulk density of the granular solids

ρ_l = density of flowing liquid

ρ_r = particle density of the solids

σ_r = radial normal stress

$(\sigma_r)_w$ = normal radial stress at the wall

$(\sigma_r)_{w^*}$ = normal radial stress at the wall for a material with no internal friction

σ_z = normal vertical stress

$(\sigma_z)_a$ = average vertical stress across the bed

τ = shear stress acting in a plane parallel to the stress

τ_{rz} = shear stress in vertical direction resulting from a radial force

$(\tau_{rz})_w$ = τ_{rz} at the tube wall

Subscripts

d = value of stress in deep beds, that is the asymptotic value in concurrent movement

o = value of stress at zero bed depth

LITERATURE CITED

1. Delaplaine, J. W., *A.I.Ch.E. Journal*, **2**, 127 (1956).
2. Hancher, C. W., and S. Jury, *Chem. Eng. Prog. Symposium Ser. 24*, **55**, 87 (1959).
3. Janssen, H. A., *Z. Ver. Deut. Ing.*, **39**, 1045 (1895).
4. Jenike, A. W., "Gravity Flow of Bulk Solids," Utah Engineering Experiment Station, University of Utah, Bul. 108 (1961).
5. Ketchum, M. S., "The Design of Walls, Bins, and Grain Elevators," McGraw-Hill, New York (1919).
6. Pleissner, J., *Z. Vert. Deut. Ing.*, **50**, 976 (1906).
7. Tschebotarioff, G., "Soil Mechanics, Foundations, and Earth Structures," McGraw-Hill, New York (1951).
8. Zenz, F. A., *Petrol. Refiner*, **36**, 173 (April, 1957).

Manuscript received November 5, 1962; revision received May 21, 1963; paper accepted June 7, 1963. Paper presented at A.I.Ch.E. Buffalo meeting.